J. Plasma Physics (2004), *vol.* 70, *part* 5, *pp.* 625–634.
DOI: 10.1017/S0022377804002879 Printed in the United Kingdom

Electron acceleration by the short pulse laser in inhomogeneous underdense plasmas

LIHUA CAO[1], WEI YU[2], HAN XU[2],
CHUNYANG ZHENG[1], ZHANJUN LIU[1] and BIN LI[1]

[1]Institute of Applied Physics and Computational Mathematics, PO Box 8009, Beijing 1000088, China
(cao_lihua@iapcm.ac.cn)

[2]Shanghai Institute of Optics and Fine Mechanics, Shanghai 201800, China

(Received 10 November 2003 and accepted 5 December 2003)

Abstract. Electron acceleration by the ponderomotive force of a laser pulse with duration less than the plasma wavelength in inhomogeneous underdense plasmas is studied by two-dimensional relativistic parallel particle-in-cell (PIC) code. Particular attention is paid to the mechanism of electron acceleration associated with the increasing group velocity of the laser pulse. In an underdense plasma layer with linearly descending density profile, the accelerated electrons move together with the laser pulse which propagates with increasing group velocity. In an inhomogeneous pre-plasma with linearly ramping density profile, as the incident laser propagates up the density gradient with decreasing group velocity, ponderomotive acceleration is reduced compared with the uniform pre-plasma. As the reflected laser propagates down the density gradient with increasing group velocity, the ponderomotive acceleration by the reflected laser is more effective due to increasing group velocity of the reflected light and the return currents induced by the incident laser light. Relativistic electrons with multi-tens-MeV energies are generated.

1. Introduction

Electron acceleration has received considerable attention in recent years in the fields of laser fusion [1–2], laser–plasma accelerators [3,4] and the generation of fast ions [5–7]. The plasma wave is driven by the ponderomotive force associated with the laser pulse. It pushes electrons ahead of the pulse, resulting in charge separation and the associated electrostatic field. This field pulls electrons back, resulting in electron oscillations behind the pulse, creating a plasma wave with phase velocity approximately equal to the group velocity of the pulse. There exits an optimum condition for wake generation which is related to the pulse duration and the plasma wavelength; the relationship between them has been proposed theoretically and experimentally [8–10]. Direction electron acceleration by the laser ponderomotive force emerges when the laser duration is much less than the optimum width the laser pulse traps the electrons and carries them with it as a soliton-like system, which was also studied in a uniform pre-plasma [11], in which the laser propagates with constant group velocity and the momentum and density distributions of the accelerated electrons remain unchanged. In a real situation, a low-density plasma is always set up at the front of a solid target with a naturally present or deliberately

created repulse so that the pre-plasma has an inhomogeneous density profile. A noticeable electron acceleration mechanism will appear due to the increasing group velocity of the laser pulse in such an inhomogeneous plasma.

The mechanism is studied in two kinds of preformed underdense plasmas with linearly descending and ascending density profiles by the 2d3v particle-in-cell (PIC) code under a distributed-memory parallel environment [12], which can work more efficiently than the code used in our previous work [13–15]. A circularly polarized, Gaussian shape laser pulse with peak intensity 5×10^{19} W cm^{-2}, wavelength $\lambda = 1$ μm and pulse duration $5T_{\text{laser}}$, is incident normally on a preformed plasma, corresponding to a cycle time of $T_{\text{laser}} \sim 3$ fs. The $v \times B$ effect can be minimized for circularly polarized lasers and the preformed plasma density is set much less than the critical value to avoid instabilities and strong electrostatic fields. Initial velocities for both electrons and ions have Maxwellian distributions with temperatures of 1 keV for electrons and $\frac{1}{3}$ keV for ions. We use a spatial mesh of 512×512 cells with 10^7 electrons and the same for the ions and they are initially filled in the simulation box to form a definite density profile and move in the x–y plane, whereas the laser propagates in the x-axis. The ions are protons with mass $M = 1836$ m and $Z = 1$.

In this paper, we first discuss the electron acceleration due to the increasing group velocity of the laser pulse in a pre-plasma with linearly descending density, then the propagation of incident and reflected laser pulses and the electron ponderomotive acceleration are investigated in an inhomogeneous preformed plasma with linearly ascending density profile.

2. Plasma with linearly descending density profile

In order to gain more insight into the electron acceleration due to the increasing group velocity of a laser pulse, we have assumed delicately the preformed underdense plasma with initial linearly descending profile from $10^{-3}n_{\text{c}}$ to 0 in the distance 20λ, where n_{c} is the critical density. So, the effect of increasing group velocity can be extruded in such an imaginary density profile. Two vacuum gaps, both with lengths 10λ, are assigned at the left and right boundaries, so the simulation box is 40λ long and 30λ in width. The reflectless boundary is chosen at the right boundary for electromagnetic fields and the calculation will continue until the incident laser pulse reaches the right boundary of the simulation box.

The dispersion relation for a light wave in a plasma is $\omega^2 = \omega_{\text{pe}}^2 + k^2c^2$, and its group velocity is

$$v_g = d\omega/dk = c\sqrt{1 - \frac{\omega_{\text{pe}}^2}{\omega^2}} = c\sqrt{1 - \frac{n_{\text{e}}}{n_{\text{c}}}},$$

where c and n_{e} are respectively the speed of light in vacuum and the electron density of plasma; the relativistic effect is not included here. Apparently, a laser pulse will propagate with increasing velocity in such a fictitious plasma.

Some temporal parameters on the laser propagation can be achieved in the simulation. At time $10T_{\text{laser}}$, the light comes to the vacuum–plasma interface where the plasma density is $10^{-3}n_{\text{c}}$, then it will travel forwards with increasing group velocity in the underdense plasma with descending density. As the laser propagates down the density gradient, the electrons are drivenforward at the ascending front of laser

https://doi.org/10.1017/S0022377804002879 Published online by Cambridge University Press

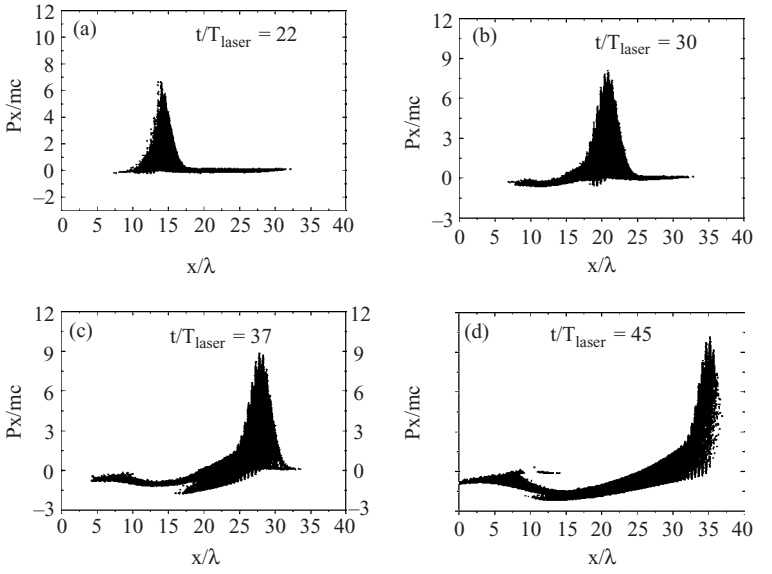

Figure 1. Electrons in phase space (x, Px) at $t/T_{\text{laser}} =$ (a) 22, (b) 30, (c) 37 and (d) 45.

pulse and backwards at the descending front. This is known as the ponderomotive force, and its magnitude is determined by the slope of the laser intensity. The pulse is so intense and so short (its duration covers only five laser periods), that the force is gigantic. Figure 1 illustrates the electrons in phase space (x, Px) at different moments. Obviously, a group of electrons are accelerated ponderomotively and move together with the laser pulse, which leaves behind a space-charge field and hence a return current which can be seen in Figs. 1(c) and 1(d). This situation continues as the laser pulse comes to the right vacuum gap, then the energetic electrons leave the plasma to the gap together with the laser pulse, as shown in Fig. 1(d).

A spike-shaped electron density profile is formed by the laser ponderomotive force since the laser enters into the preformed plasma and goes together with the pulse, while the peak density of the ponderomotively accelerated electrons decreases with time. Figure 2 shows four snapshots of the density profile as it evolves from its initial linear descending profile. The peak densities are, respectively, $2.19 \times 10^{-3} n_{\text{c}}$, $1.88 \times 10^{-3} n_{\text{c}}$, $1.12 \times 10^{-3} n_{\text{c}}$ and $4.56 \times 10^{-4} n_{\text{c}}$ at times $t/T_{\text{laser}} = 22$, 30, 37 and 45, and the corresponding group velocities of the laser in a plasma with such electron densities can be estimated to be $0.9989c$, $0.9991c$, $0.9994c$ and $0.9998c$ according to the expression above. This indicates that the laser propagates with increasing group velocity, and the highest momentum of the ponderomotively accelerated electrons increases with time as plotted in Fig. 1.

Figure 3 shows the time dependence of the electron maximum kinetic energy, where γ is the relativistic factor; three diagnostic temporal parameters on the laser peak touching the boundaries are also marked. The maximum electron kinetic energy keeps increasing after the laser impinges upon the left plasma boundary with electron density $10^{-3} n_{\text{c}}$, approaches $11mc^2$ when the pulse meets the right plasma boundary and continues to rise while traveling in the right vacuum gap until the pulse runs into the right boundary of the simulation box. This is convictive evidence

https://doi.org/10.1017/S0022377804002879 Published online by Cambridge University Press

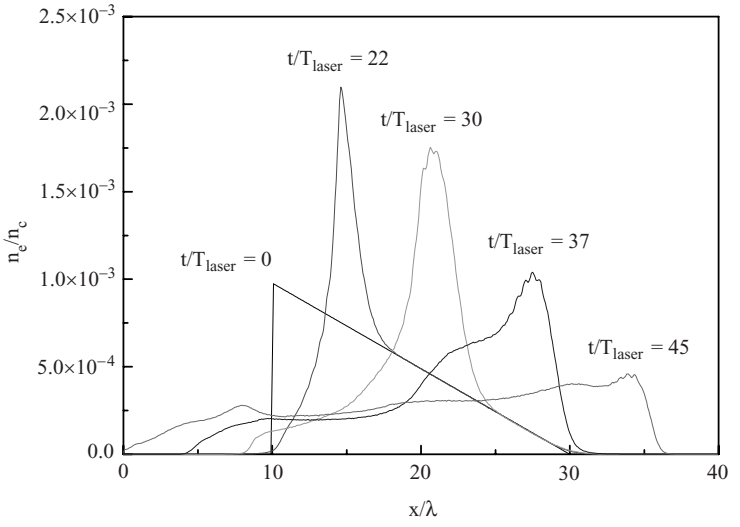

Figure 2. Snapshots of electron density profiles at $t/T_{\text{laser}} = 22$, 30, 37 and 45; the initial electron density profile is overlapped.

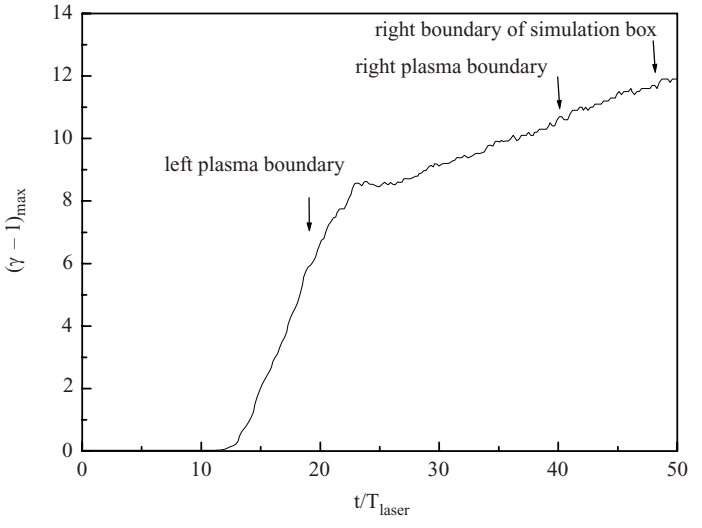

Figure 3. Time dependence of the maximum kinetic energy of electrons until the laser pulse touches the right boundary of the simulation box.

of the electron ponderomotive acceleration by the laser pulse with increasing group velocity.

3. Inhomogeneous preformed plasma

A preformed underdense plasma with linearly rising profile is assumed in the following discussion. This kind of plasma profile is easily set up in experiments

https://doi.org/10.1017/S0022377804002879 Published online by Cambridge University Press

and closer to the real situation. The particle simulation presented shows that the electrons accelerated in the underdense plasma have larger momentums than those generated in the overdense zone [16]. In order to focus on the propagations of incident and reflected light in the underdense pre-plasma, we do not consider the forward energetic electrons which will move into or through the solid target. The surface of solid target is abstracted to a perfect conductor boundary and the laser pulse will be ejected entirely as it touches the right boundary of simulation box. A vacuum gap with length 10λ between the incident surface of the laser pulse and the preformed plasma is assigned to allow the plasma to expand and the reflected laser pulse to propagate, so the simulation box is 30λ long and 30λ wide. The initial density profile of the plasma ramps linearly from 0 to $10^{-3}n_c$ in the distance 20λ. The simulation reveals that the laser pulse goes forward after entering into the pre-plasma at $10T_{laser}$, is reflected and propagates backwards after $40T_{laser}$, and the traveling reflected light comes to the vacuum–plasma surface again at $60T_{laser}$.

PIC simulation gives details of the evolution of the electron density profile from its initial linear profile. A 'peaky' density profile is built up by the tremendous laser ponderomotive force and moves forwards with the incident light which propagates with decreasing group velocity, while the peak density increases with time as displayed in Fig. 4(a). However, it returns with the reflected laser traveling with increasing group velocity after the laser pulse is rebounded by the right boundary, while the electron peak density decreases with time as shown in Fig. 4(b). The group velocities of the laser pulse can be estimated to be $0.9998c$, $0.9993c$ at $t/T_{laser} = 22$, 30 and $0.99952c$, $0.99954c$, $0.99959c$, 0.99975 at $t/T_{laser} = 44$, 52, 60, 67 from the diagnosis of the peak electron density.

As the incident laser propagates up the density gradient with decreasing group velocity, the ponderomotive acceleration is reduced compared with uniform pre-plasma and the peak momentum of accelerated electrons slightly increases as shown in Fig. 5(a). As the reflected laser propagates down the density gradient with increasing group velocity, the ponderomotive acceleration is greatly enhanced. A group of electrons carry increasing negative peak momentum with time, and it keeps rising even after the reflected laser pulse moves beyond the initial pre-plasma–vacuum boundary as shown in Fig. 5(b). At time $67T_{laser}$, the pulse can propagate with group velocity close to the speed of light in vacuum when it is near the left boundary of the simulation box, and highly accelerated electrons with the highest momentum exceeding -80 can be trapped by the reflected pulse, although their number are so few. These strong backward-accelerated energetic electrons can be attributed to two effects. The first is the effect of increasing group velocity of the reflected laser pulse being discussed here: a small number of electrons can be trapped and carry increasing energies. The other is the pre-acceleration of the relativistic electron return current as expounded before [14], the electrons can attain even higher energies due to their longer acceleration length and their high initial momentum from a relativistic current.

A detailed diagnosis of energetic electrons is carried out in our simulations in order to acquire deeper insight into the new mechanism of electron acceleration. The maximum kinetic energy of electrons grows continuously as exhibited in Fig. 6. This indicates that the electrons can undergo three successive nonlinear acceleration processes: they can be driven by the incident laser pulse during the period $10T_{laser}$–$32T_{laser}$, by the standing-wave between times $32T_{laser}$ and $40T_{laser}$, and by

https://doi.org/10.1017/S0022377804002879 Published online by Cambridge University Press

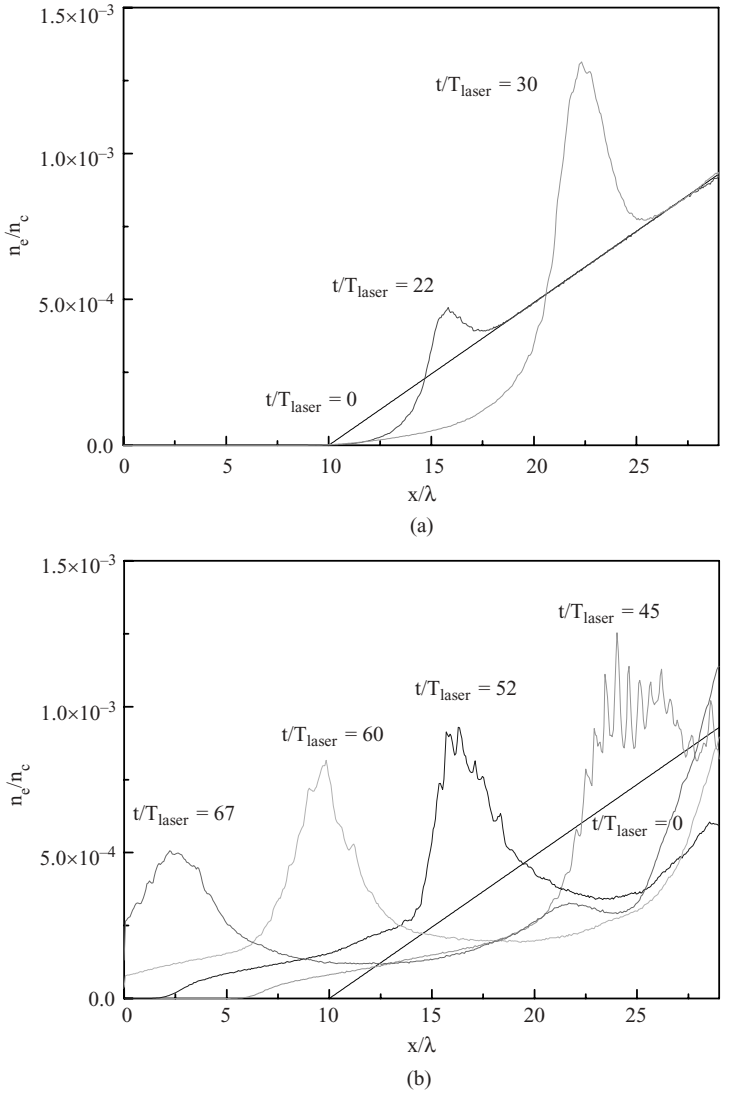

Figure 4. Evolutions of electron density profiles: (a) as the incident laser propagates up the density gradient at $t/T_{\text{laser}} = 22$ and 30: (b) as the reflected laser propagates down the density gradient at $t/T_{\text{laser}} = 45$, 52, 60 and 67; the initial electron density profile is also overlapped.

the reflected pulse after $40T_{\text{laser}}$. The standing wave can heat electrons with a highest kinetic energy of $35mc^2$; higher energy electrons with energies greater than $40mc^2$ can only be created after the laser pulse is reflected and propagates backwards in the underdense plasma. The electrons with energies greater than $60mc^2$ only begin to emerge when the reflected pulse travels near the left vacuum gap. The maximum kinetic energy approaches to $82mc^2$ or 41 MeV. So the energy from the acceleration of the reflected laser pulse is several times higher than that by the standing-wave and the conventional ponderomotive force. The increasing rate of the maximum

https://doi.org/10.1017/S0022377804002879 Published online by Cambridge University Press

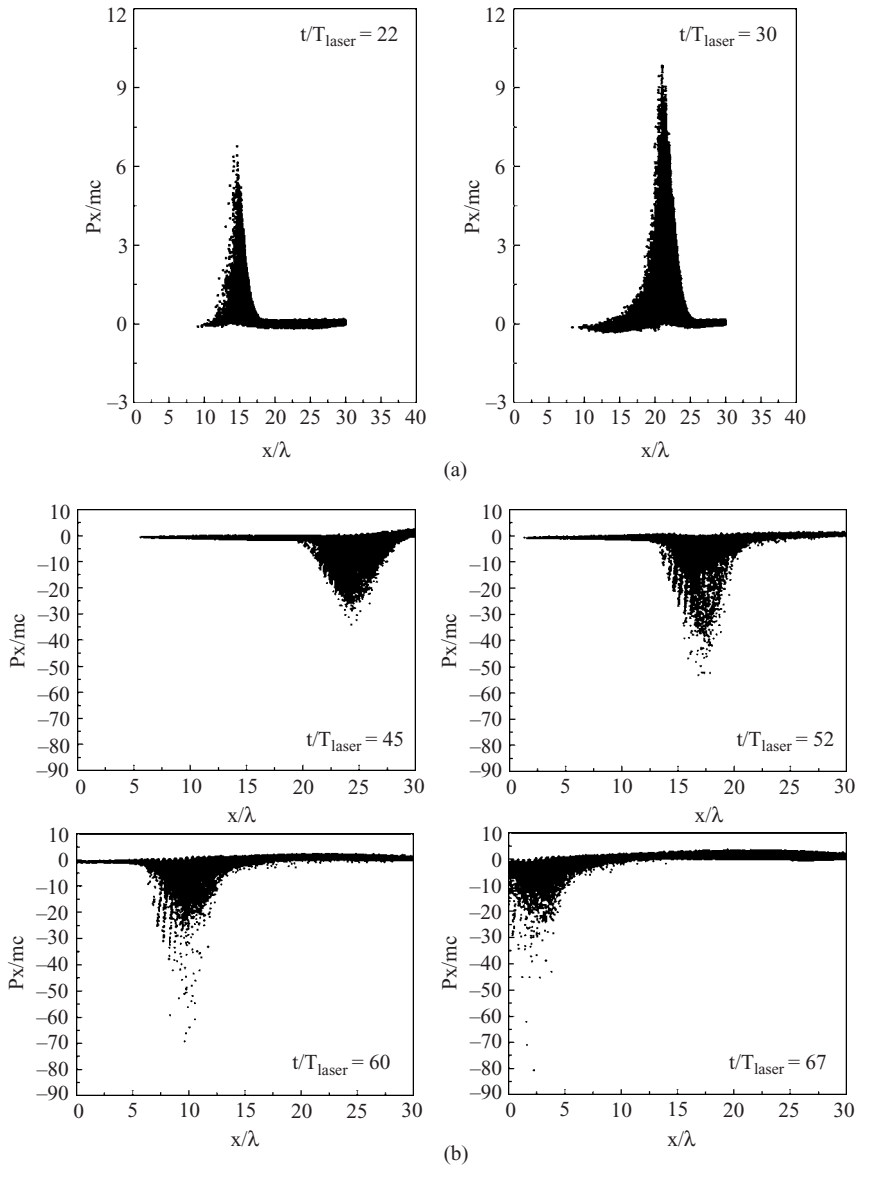

Figure 5. Snapshots of electrons in phase space (x, Px): (a) when the incident laser propagates forwards at $t/T_{\text{laser}} = 22$ and 30; (b) when the reflected laser travels backwards at $t/T_{\text{laser}} = 45$, 52, 60 and 67.

electron kinetic energy in the process of a reflected laser pulse propagating in the pre-plasma is greater than that of incident laser traveling, which can be seen clearly from Fig. 6. It is further strong evidence of electron ponderomotive acceleration due to the increasing group velocity of a laser pulse.

To further illustrate the process of electron acceleration, we diagnosed the evolutions of the number and average kinetic energy of three groups of energetic electrons with $\gamma - 1$ greater than 20, 40 and 60. In an underdense preformed plasma with

https://doi.org/10.1017/S0022377804002879 Published online by Cambridge University Press

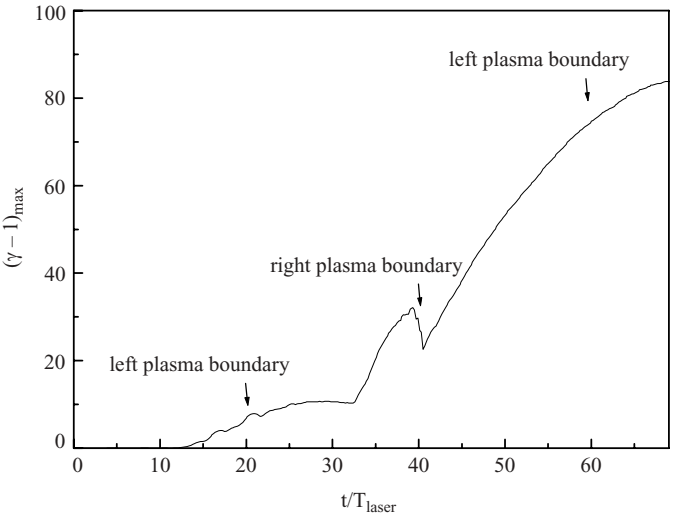

Figure 6. Time evolution of the maximum electron kinetic energy.

ramping density profile, even if the highest energy of accelerated electrons increases with time, the number of energetic electrons will rise at first and then fall as shown in Fig. 7(a). This is because the reflected laser pulse travels backwards with increasing group velocity, thus it becomes harder to trap electrons and there are fewer and fewer electrons which can come up with the pulse. However, the electron energy is very high once it is trapped, so the average energy of energetic electrons still increases continuously with time, even though their number has begun to descend as described in Figs. 7(a) and 7(b).

The simulation box limits the distance over which electrons can effectively gain energy from the reflected laser pulse. The calculation has to be ended as the reflected light reaches the left boundary, but it could be imagined that the maximum kinetic energy would keep rising until there is no electron which can be trapped anymore if the simulation box was long enough. The longer the acceleration distance, the greater the kinetic energy of the accelerated electrons.

4. Conclusions

In conclusion, strong evidence for another new mechanism of electron acceleration by increasing the group velocity of a laser pulse has been presented. Electron acceleration by the laser ponderomotive force in inhomogeneous pre-plasma differs from that in uniform pre-plasma. An inhomogeneous pre-plasma with linearly ascending density profile enables more efficient ponderomotive acceleration by the reflected laser because of two effects. The first is the increasing group velocity of the laser pulse and the other is the relativistic return currents. The reflected light travels down the density gradient with increasing group velocity and will accelerate some electrons to higher energies. The return-current electrons accelerated by the reflected pulse can be even more energetic because of their high initial momentum and longer acceleration path. Electrons with multi-tens-MeV can be produced by

https://doi.org/10.1017/S0022377804002879 Published online by Cambridge University Press

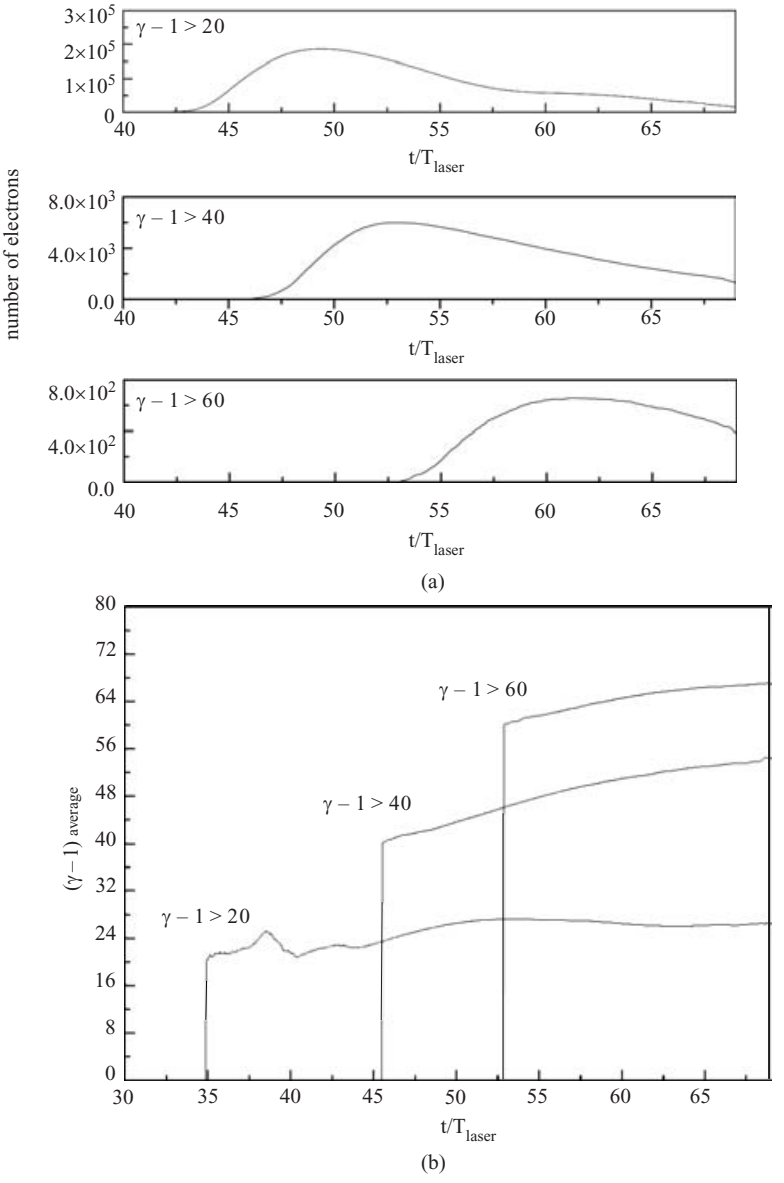

Figure 7. Time evolutions of: (a) the number of electrons; and (b) their average kinetic energy for electrons with $\gamma - 1$ greater than 20, 40 and 60.

the reflected laser pulse, and their average energy increases with time although their number decreases with time.

Acknowledgements

We gratefully acknowledge the support of the National High Technology ICF Committee in China, the Foundation of the China Academy of Engineering and Physics (2000 Z0206) and the National Natural Science Fund of China (10135010 and 10085002).

References

[1] Suckewer, S. and Skinner, C. H. 1990 *Science* **247**, 1553.
[2] Tabak, M. et al. 1994 *Phys. Plasmas* **1**, 1626.
Delamater, N. D. et al. 1996 *Phys. Plasmas* **3**, 2022.
Pawley, C. J. et al. 1997 *Phys. Plasmas* **4**, 1969.
[3] Modena, A. et al. 1995 *Nature* **377**, 606.
[4] Umstadter, D. et al. 1996 *Science* **273**, 472.
[5] Mackinnon, A. J. et al. 2002 *Phys. Rev. Lett.* **88**, 215 006.
[6] Badziak, J. et al. 2001 *Phys. Rev. Lett.* **87**, 215 001.
[7] Clark, E. L. et al. 2000 *Phys. Rev. Lett.* **85**, 1654.
[8] Tajima, T. and Dawson, J. M. 1979 *Phys. Rev. Lett.* **43**, 267.
[9] Yu, M. Y. et al. 2003 *Phys. Plasmas* **10**, 2468.
[10] Hamster, H. et al. 1993 *Phys. Rev. Lett.* **71**, 2725.
[11] Wei Yu et al. 2000 *Phys. Rev. Lett.* **85**, 570.
[12] Xu Han et al. 2002 *Chinese Journal of Computational Physics*, **19**, 305 (in Chinese).
[13] Lihua Cao, Wenwei Chang and Zongwu Yue 1998 *Phys. Plasmas* **5**(2), 499.
[14] Lihua Cao, Tieqiang Chang, Wenwei Chang and Zongwu Yue 2001 *J. Plasma Phys.* **65**, 353.
[15] Cao Lihua, Liu Zhiyong, Chang Wenwei and Yue Zongwu 2001 *Chin. Phys. Lett.* **18**, 1095.
[16] Yan Xin et al. 2003 *Phys. Scr.* **67**, 544.